

# Air-sea interaction through waves

Peter A.E.M. Janssen

*ECMWF  
Shinfield Park  
Reading, U.K.  
p.janssen@ecmwf.int*

## ABSTRACT

At ECMWF suggestions emanating from the 1970's regarding the sea state dependence of air-sea fluxes have been followed up by introducing a coupled ocean-wave, atmosphere model into operations in 1998. The properties of the ECMWF air-sea interaction model in extreme conditions and extensions towards the determination of the heat flux and the ocean mixed layer are briefly discussed.

## 1 Introduction

At ECMWF there is slow but steady progress in the development of a fully-coupled *atmosphere, ocean-wave, ocean circulation model*, simply called the Integrated Forecasting System (IFS). In June 1998 we introduced the first operational coupled atmosphere, ocean-wave model, which was followed by the first version of the IFS (atm-ocw-oc), used for seasonal forecasting and later for monthly forecasting. An overview of the main applications of the coupled system may be found in Fig. 1.

Presently, the interactions between the several components are as follows: Momentum loss and heat exchange from the atmosphere depend on the sea state following the approach of Janssen (1991 and 2004). The ocean circulation is driven by the sea state dependent fluxes and produces surface currents which are returned to the atmospheric model needed for the determination of the fluxes.

As a next step, following O. Saetra's work (Saetra *et al*, 2007) we are going to test impact of effects such as *Stokes-Coriolis* forcing and it is proposed to drive the ocean circulation model with momentum and energy fluxes directly from the wave model. In addition, effects of ocean-wave, current interaction will be introduced.

In this short paper the following items are briefly discussed:

- **MOMENTUM FLUX FOR EXTREME WINDS**

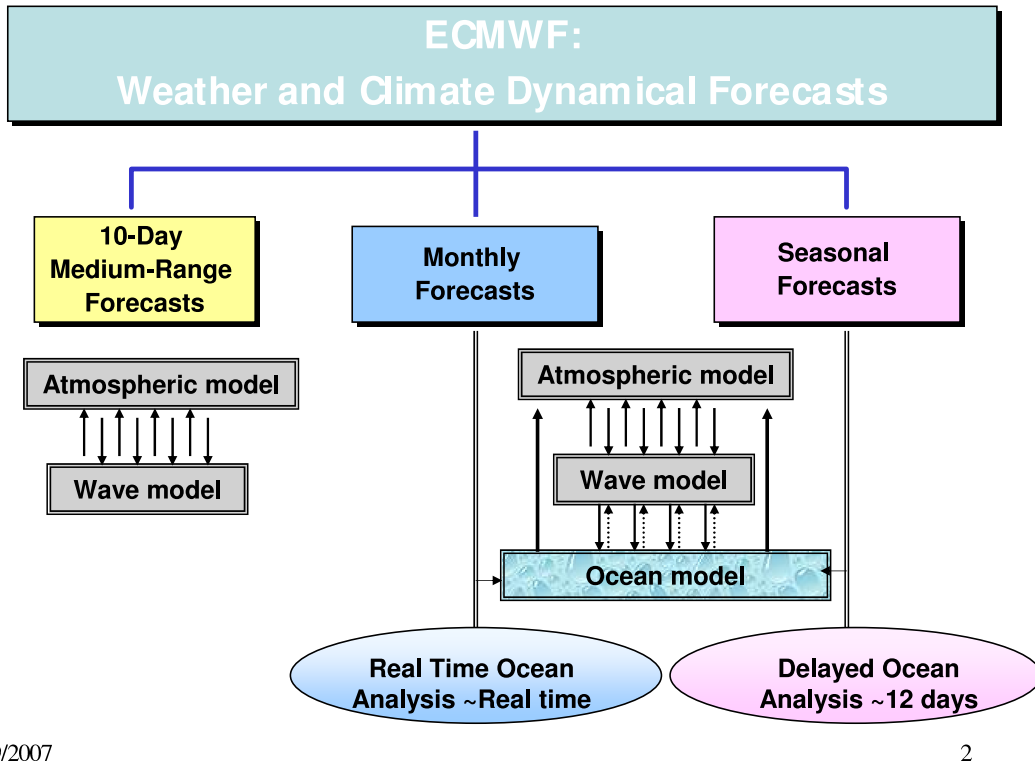
For extreme winds a maximum in the drag coefficient is found. Illustrated with one example from hurricane Katrina using  $T_{799}$  version of the IFS.

- **HEAT FLUXES AND SEA STATE**

Determine effects of growing ocean waves on heat flux according to critical layer theory. Gives a Dalton and Stanton number which increases with wind speed. This is at variance with the results from HEXOS, but not with recent measurement campaigns. Results in a deepening of hurricane Katrina by 10-15 mb.

- **WAVE BREAKING AND MIXED LAYER**

Energy flux  $\Phi_{oc}$  from atmosphere to ocean is controlled by wave breaking. Gives an energy flux of the type  $\Phi_{oc} = m\rho_a u_*^3$  where  $m$  depends on the sea state.



8/29/2007

2

Figure 1: Overview of operational applications with the coupled system.

## 2 Air-sea interaction model and extreme winds

### 2.1 The problem

Using a simple model for a hurricane, Emanuel argued that central pressure and maximum wind speed depend on the ratio of enthalpy to momentum exchange coefficients,  $C_k/C_D$ . According to Emanuel(1995) this ratio should lie in the range 1.2 – 1.5 in order to get a realistic simulation of a hurricane. However, according to HEXOS (DeCosmo *et al.*, 1996),  $C_k$  (which is the Dalton or Stanton number) is independent of wind speed while  $C_D$  increases with wind speed, hence the ratio  $C_k/C_D$  decreases with increasing windspeed thereby seriously limiting the maximum wind speed of a hurricane. But these exchange coefficients have only been observed up to a wind speed of 20 m/s, hence extrapolation to extreme cases is most likely problematic. There are a few ways out of this. The drag coefficient gets a *maximum* for increasing wind and/or the heat flux *increases* with windspeed.

### 2.2 The air-sea interaction model

Before results are discussed I will first give a basic air-sea interaction model, details of which are given in Janssen (1991 and 2004). Ocean waves, described by the wave spectrum  $F(\mathbf{k}; \mathbf{x}, t)$ , are governed by the *energy balance equation* (Komen *et al.*, 1994)

$$\frac{D}{Dt}F = S = S_{in} + S_{nl} + S_{ds}, \quad (1)$$

and the source functions  $S$  represent the physics of wind input, dissipation by wave breaking and nonlinear four-wave interactions. In the ECMWF formulation, the Charnock parameter  $z_0^* = gz_0/u_*^2$  (with  $z_0$  the roughness

length and  $u_*$  the friction velocity) is given by

$$z_0^* = \frac{gz_0}{u_*^2} = \frac{\alpha}{\sqrt{1 - \frac{\tau_w}{\tau}}}, \alpha \simeq 0.01 \quad (2)$$

and depends on the ratio of wave-induced stress  $\tau_w$  to total stress  $\tau$ , where

$$\tau_w = \left. \frac{\partial \mathbf{P}}{\partial t} \right|_{wind} = \int d\omega d\theta \frac{\mathbf{k}}{\omega} S_{in}. \quad (3)$$

In the present coupled system at every atmospheric time step (for example with the  $T_{799}$  model the time step is 720 s) neutral wind fields, air density fields and a gustiness factor are passed from the atmospheric model to the wave model. Then the wave model integrates one time step and determines the two-dimensional wave spectrum according to the energy balance equation (1). The wave-induced stress is obtained from Eq. (3) which is followed by a determination of the Charnock parameter field  $z_0^*$ . The loop is closed by passing the Charnock field to the atmospheric model which then continues with the next time step by using the updated Charnock field in the surface drag over the oceans. Here, the neutral drag coefficient  $C_D$  is given by

$$C_D(L) = \left\{ \frac{\kappa}{\log(L/z_0)} \right\}^2. \quad (4)$$

with  $L$  the height in the surface layer,  $\kappa$  is the von Kármán constant and  $z_0 = z_0^* u_*^2 / g$ .

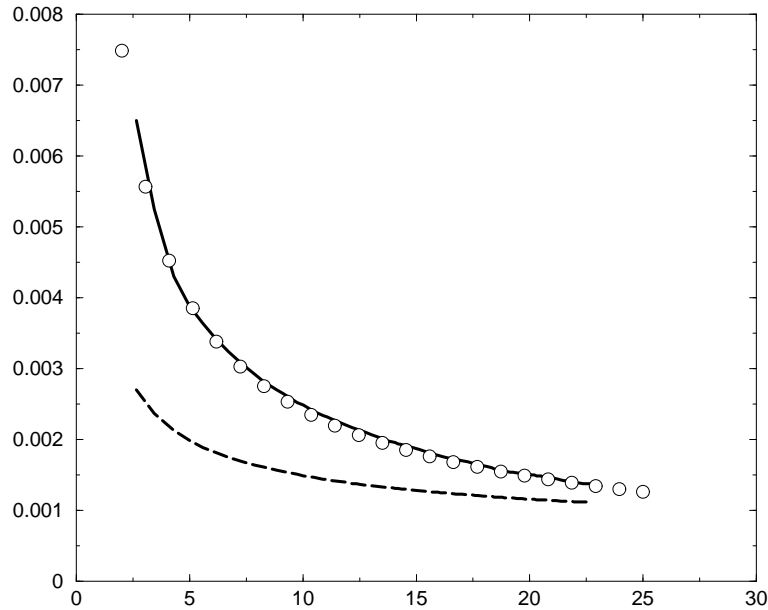


Figure 2: Comparison of simulated and parametrized relation of drag coefficient  $C_D(\lambda_p/2)$  versus wave age  $c_p/u_*$ . Black line: simulation; open circles Eq. (5), and dashed line is the case of constant parameter ( $z_0^* = 0.01$ ).

The sea state dependence of the air-sea momentum transfer is measured in terms of the wave age parameter  $c_p/u_*$ . Since the JONSWAP campaign (Hasselmann *et al.* 1973) it is known that a good parameter to characterize the stage of development of windsea is the wave age parameter, where 'young' windsea has a typical value  $c_p/u_* \simeq 5 - 10$  while old windsea has wave ages larger than 30. There have been several attempts in the past to find observational evidence for the wave age dependence of the Charnock parameter in the special case of windsea generation. Examples are: 1) Donelan (1982) who studied wind wave generation and the sea

state dependent drag for the short fetches of lake Ontario, and 2) Smith *al.* (1992) who studied the air-sea transfer during the HEXOS campaign, which took place in the southern bight of the North Sea. However, objections were raised against the findings of Donelan (1982) and Smith *al.* (1992) because of the problem of spurious correlation. At a particular measurement site the range of phase velocities  $c_p$  is usually limited compared to the range of friction velocities and as a result, based on observations from one measurement site, an empirically obtained relation between the Charnock parameter and the wave age may be spurious because it is in essence a relation between the Charnock parameter and the friction velocity. A way to avoid the problem of self-correlation is to combine observations from a number of measurement campaigns so that the range of phase velocities is increased. This approach was followed by Hwang (2005). In addition, rather than obtaining a parametrization for the Charnock parameter, which is sensitive to errors in observed friction velocity, Hwang sought a relation between the drag coefficient and the wave age. The usual reference height for the drag coefficient is 10 m, but Hwang argued that from the wave dynamics point of view a more meaningful reference height should be proportional to the wavelength  $\lambda_p$  of the peak of the wave spectrum. Using wavelength scaling Hwang (2005) found

$$C_D(\lambda_p/2) = A (c_p/u_*)^a \quad (5)$$

with  $A = 1.220 \times 10^{(-2)}$  and  $a = -0.704$ , reflecting the notion that the airflow over young windsea is rougher than over old windsea. It is emphasized that the parametrization (5) for the drag coefficient is not valid for extremely young windseas, hence (5) only holds for windseas with  $c_p/u_* > 5$ . As shown in Fig. 2 the present formulation of the interaction between wind and waves gives, compared to Hwang's parameterization (5) a realistic representation of the drag coefficient at half the peak wavelength.

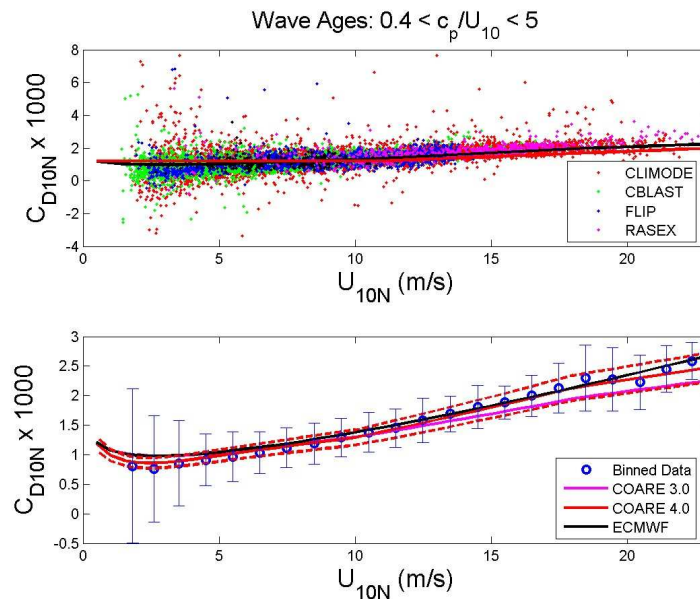


Figure 3: Comparison of mean drag relation versus neutral wind according to Coare 3.0 and a newly proposed Coare 4.0 algorithm (J. Edson, this workshop) with the mean drag relation according to the ECMWF model.

Therefore, for windsea it is possible to obtain a convincing parametrization of the sea state dependence of the surface stress. However, under mixed-sea conditions the drag coefficient and the dynamic roughness are difficult to validate at this stage. In stead, the statistical properties of the present air-sea interaction module have been validated. Hans Hersbach collected on the global domain for the year 2005 model drag coefficients and surface wind speeds and he found that on average the drag was the following function of neutral wind speed at

10 m height:

$$C_D(10) = (a + bU_{10}^{p_1}) / U_{10}^{p_2} \quad (6)$$

where  $a = 1.0310^{-3}$ ,  $b = 0.0410^{-3}$ ,  $p_1 = 1.48$  and  $p_2 = 0.21$ . In Fig. 3 (obtained from J. Edson, see also this workshop for a detailed discussion of the observations) the average model relation for the drag is compared with bin-averaged observations from a few recent observation campaigns and with a corresponding fit to the data according to the newly proposed Coare 4.0 algorithm. The agreement between model and the Coare 4.0 algorithm is good. Note that the Fig. also shows the present Coare 3.0 algorithm which differs significantly from the Coare 4.0 result because the present algorithm is only based on observations of the stress up to a neutral wind speed of 18 m/s, and is therefore thought to be less reliable in the high wind speed regime.

### 2.3 Extreme winds

Hurricane winds are highly variable in space and time, and therefore the sea state is extremely young ( $c_p/u_* < 5$ ). In those circumstances there are relatively few waves to exert a stress on the airflow and as a consequence the airflow is smooth. In the course of time more and more waves are generated resulting in an increase in roughness and the drag until the waves get so steep that wave breaking and nonlinear interactions *limit and reduce the roughness*. This picture is confirmed by Fig. 4 (from Caulliez et al. (2008) but see for an earlier discussion of this topic Komen *et al.* (1998)) which shows the observed Charnock parameter  $z_0^*$  as function of the inverse of the wave age  $u_*/c_p$ .

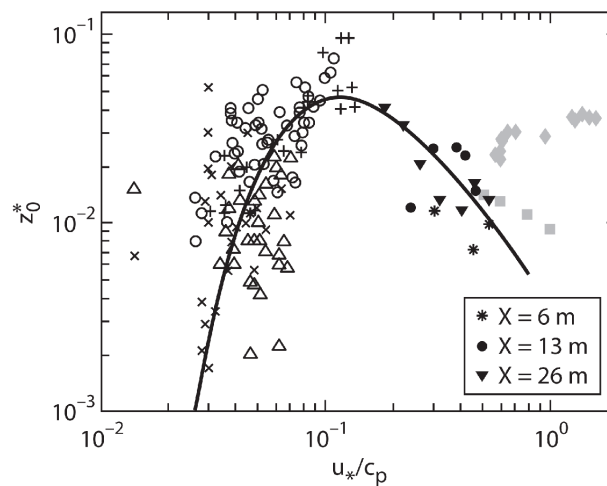


Figure 4: Charnock parameter  $z_0^*$  as function of the inverse wave age  $u_*/c_p$ . Note the maximum value of the Charnock parameter in the range 5-10. The data to the left of the maximum are from field campaigns while the data to the right of the maximum are based on laboratory experiments (from Caulliez et al. 2008).

For extremely young windseas (say  $c_p/u_* < 5$ ) the Charnock parameter has low values of the order of 0.01, and in this range of wave ages the Charnock parameter increases with wave age until a maximum value of about 0.1 is reached. For larger wave ages ( $c_p/u_* > 5 - 10$ ) the Charnock parameter decreases with wave age in agreement with the findings of a number of observational campaigns in the 1980's and 1990's and in agreement with the fit to observations given in Eq. (5). The fact that there is a maximum in the Charnock parameter as a function of wave age has some interesting consequences for the simulation of the drag coefficient field under hurricane conditions.

As an example I discuss the simulation of hurricane Katrina just before landfall. The simulation shown in Fig. 5 was performed with the  $T_{799}$  version of the ECMWF model and the mean sea level pressure field shows a

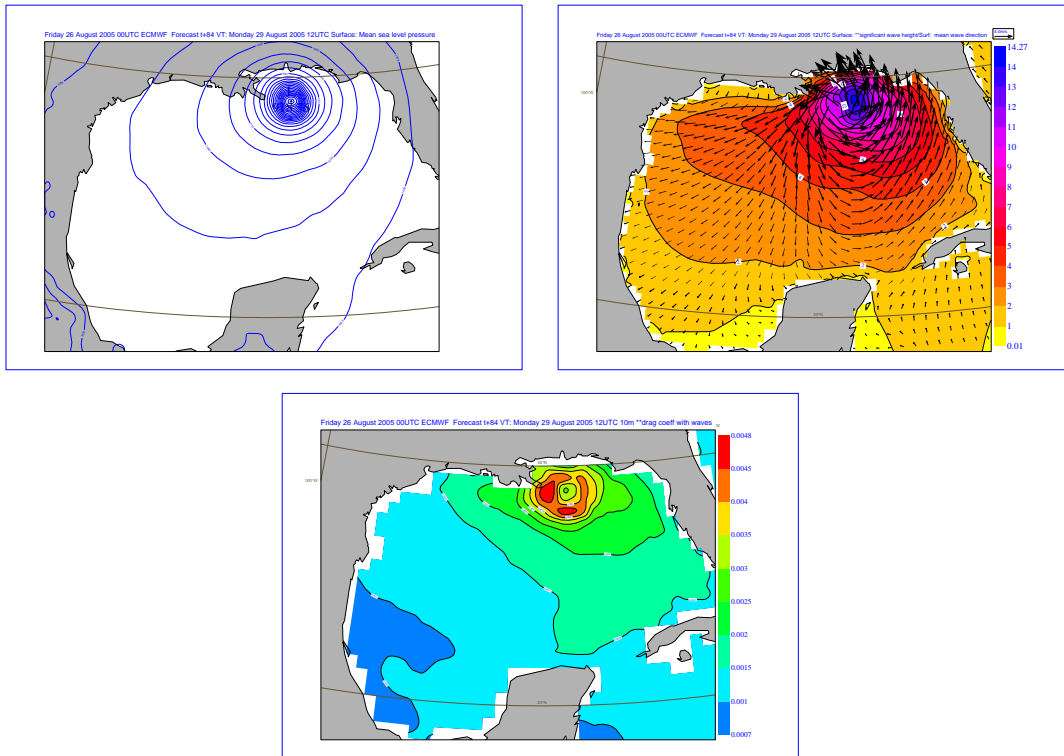


Figure 5: 84 hour forecast (valid at 2008082600 UTC) with  $T_{799}$  version of the ECMWF model of mean sea level pressure, significant wave height and drag coefficient for hurricane Katrina. Note that while the pressure field is almost symmetric, there is a clear asymmetry in the wave height field with maximum wave height to the right of the propagation direction of the hurricane. In sharp contrast to the wave height field the maximum drag is to the left of the propagation direction.

symmetric, quite deep low of 918 mb while the wave height field and the drag coefficient field are asymmetric. The reason for the asymmetry in the wave height field is easily understood when it is realized that hurricane Katrina was moving towards New Orleans with a speed of the order of 5 m/s. As a result, the forcing windfield to the right of the propagation direction is larger by 10 m/s compared to the area to the left. The consequence is that indeed the significant wave height field is expected to be the largest in the area to the right of the propagation direction of the hurricane. In contrast, according to the simulation with the coupled wave-ECMWF model, the drag coefficient field shows a maximum to the left of the propagation direction of Hurricane Katrina. Now, wave ages to the right of the low are extremely small, of the order of 3, therefore according to Fig. 4 the Charnock parameter is small, while to the left of the low, wave age is of the order of 10, giving quite large values of the Charnock parameter. This may explain why there is a maximum to the left of the low where winds are relatively low. There is no need to emphasize that for a stationary hurricane such an asymmetry does not arise.

My findings are in qualitative agreement with recent observations of a number of hurricanes as reported by Powell (2008). The height dependence of the wind profile was determined by means of drop sondes and the roughness length was obtained from the observations assuming a logarithmic wind profile. Powell's results are shown in Fig. 6, where the left panel gives the drag coefficient as function of neutral wind speed. The drag coefficient is seen to reach a maximum at about a wind speed of 40 m/s. The right panel stratifies the data according to the location of the observations with respect to the propagation direction of the low. The largest drag coefficients, being about  $4.8 \times 10^{-3}$ , are found for a wind speed of about 35 m/s in the left front sector of the hurricane.

Note that the present agreement between the ECMWF model for air-sea interaction and Powell's observations

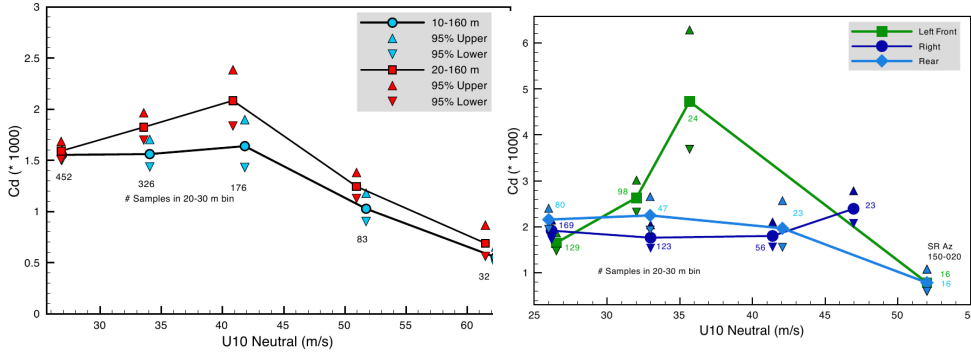


Figure 6: The left panel shows drag coefficient (squares) as function of 10 m neutral wind speed obtained from observations with drop sondes of a number of hurricanes. The surface roughness is obtained using the profile method. Upward and downward pointing triangles indicate the 95% confidence limits on the estimates. Numbers near each symbol indicate the number of wind speed samples. Two relations are shown one based on the 10-160 m layer and one based on the 20-160 m layer. Powell regards the 20-160 m layer as more representative of the lowest levels. The right panel (note the change of scale by a factor of two) stratifies the same data according to the location of the data with respect to the propagation direction of the low (from Powell (2008)).

is at best qualitative at the moment. Observing the stress in hurricane conditions is no mean feat, and it is my impression that Powell seems to underestimate the drag to some extent. This follows from a comparison of the results of the Coare 4.0 drag relation (see Fig 3). At a wind speed of 22 m/s the drag according to Coare 4.0 is around  $2.5 \times 10^{-3}$  while from Fig. 6 it follows that with high confidence the drag coefficient is  $1.6 \times 10^{-3}$  at a wind speed of 26 m/s. Assuming that in this wind speed range the drag coefficient is still increasing, I would expect a drag coefficient which is higher than the one at 22 m/s. This discrepancy is presently not well understood and more work is needed to resolve this matter.

### 3 Heat fluxes and the sea state

In this section I will assume that heat and moisture flux can be treated on an equal footing (and are equal) and I assume the passive scalar approximation, i.e. these quantities do not affect the dynamics of the flow to a significant extent. Denoting by  $\Delta T$  the air-sea temperature difference, one has

$$\Delta T = \frac{q_*}{\kappa U_*} \log(z/z_T) \quad (7)$$

where  $z_T$  is a thermal roughness length and  $q_* = -\langle w'T' \rangle$ . The Dalton number  $C_q$  then follows from

$$q_* = C_q U_{10} \Delta T_{10} \quad (8)$$

and, on elimination of  $\Delta T_{10}$ , one finds

$$C_q = C_D^{1/2} \frac{\kappa}{\log(10/z_T)}, \quad (9)$$

where  $C_D$  is the drag coefficient which increases with  $U_{10}$ . An important question to ask is to what extent  $z_T$  depends on sea state and/or wind speed.

In Janssen (1997) the theory of *wind-wave generation* was extended to include thermal *stratification*. From previous work it is found that the mean flow is affected by the waves through a diffusion term:

$$\frac{\partial}{\partial t} U_0 = \frac{\partial}{\partial z} K(z) \frac{\partial}{\partial z} U_0 + D_w \frac{\partial^2}{\partial z^2} U_0 \quad (10)$$

where  $K(z)$  denotes a turbulent eddy viscosity and  $D_w$  represents the effects of gravity waves (with wave spectrum  $F(k)$ ) on the mean flow,

$$D_w = \frac{\pi\omega^2|\chi|^2}{|c - v_g|} F(k), \quad (11)$$

with  $\omega = \sqrt{gk}$ ,  $v_g = \partial\omega/\partial k$  and  $\chi$  is the normalized vertical component of the wave-induced velocity. In fact, this approach forms the basis of the parametrization of the effect of waves on the mean flow as displayed in Eqns. (2-3).

However, for growing windsea one would expect, by analogy with transport by eddies, that the wave-induced motion in the air will enhance heat transport. In fact, in the passive scalar approximation the evolution of *mean temperature* is found to be

$$\frac{\partial}{\partial t} T_0 = \frac{\partial}{\partial z} \left\{ (K(z) + D_w) \frac{\partial}{\partial z} T_0 \right\}. \quad (12)$$

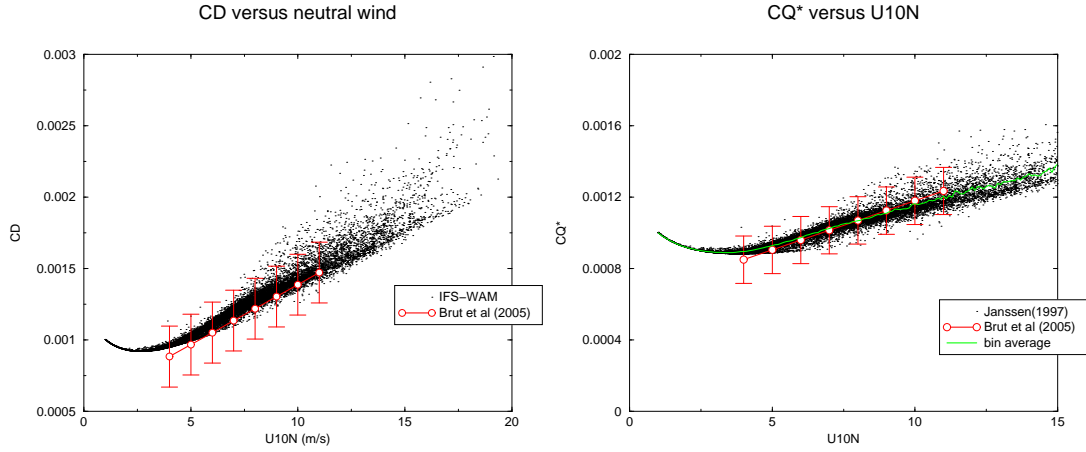


Figure 7: Comparison between a parametrization by Brut *et al.* (2005) of the drag coefficient and the Dalton number as function of wind speed with bin-averaged model equivalents obtained from one ECMWF forecast field.

By parametrizing the wave effect the wind and temperature profile can be obtained and one now immediately finds the expressions for the drag coefficient  $C_D$  and the Dalton number  $C_q$ :

$$C_D(10) = \left\{ \frac{\kappa}{\log(10/z_0)} \right\}^2, \quad C_q(10) = C_D^{1/2} \frac{\kappa}{\log(10/z_T)}. \quad (13)$$

For more details on this see Janssen (1997). It is straightforward to evaluate these coefficients from ECMWF's IFS. Results show (see Fig. 7), in agreement with Brut *et al.* (2005), an increase of  $C_D$  with wind and just as in the case of Fig. 4, the agreement between modelled drag and observed drag is impressive. Also  $C_q$  increases with wind but to a lesser extent. However, the result for  $C_q$  is in sharp contrast with HEXOS observations which gives a constant for the Dalton number. Smedman *et al.* (2007) (and also Oost *et al.* (2000)) had another look at the heat exchange problem and they found that, in agreement with Brut *et al.* (2005),  $C_q$  increases with wind speed.

### 3.1 Impact on hurricane Katrina

I have performed a number of experiments on the case of hurricane Katrina to test sensitivity to the formulation of the heat and moisture flux. The control experiment is the operational IFS which uses the following

representation of the thermal roughness

$$z_T = \delta \frac{v}{u_*}, \quad \delta = 0.4, 0.6.$$

When substituted in the expression of the Dalton/Stanton number,

$$C_q = C_D^{1/2} \frac{\kappa}{\log(10/z_T)},$$

this choice of thermal roughness results in a Dalton/Stanton number that is almost independent of wind speed (which agrees with HEXOS).

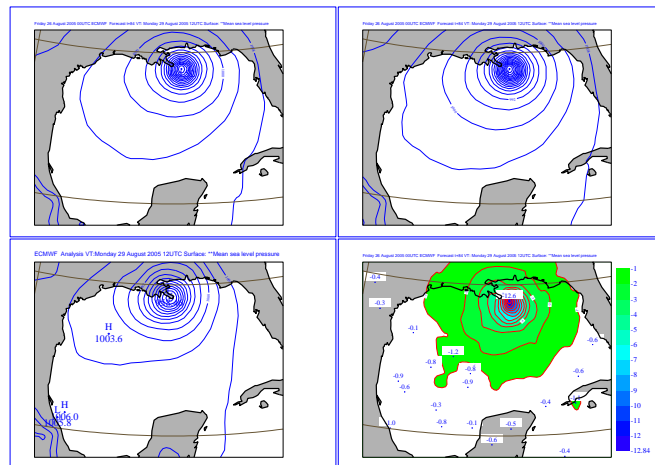


Figure 8: Impact of sea state dependent heat fluxes on the evolution of the surface pressure field for hurricane Katrina. Forecast step is 84 hours verifying on 2005082912. Upper left panel shows the control simulation, upper right panel shows the experiment and the lower right panel shows the difference between control and experiment. Sea state effects deepen the low by 10-15 mb.

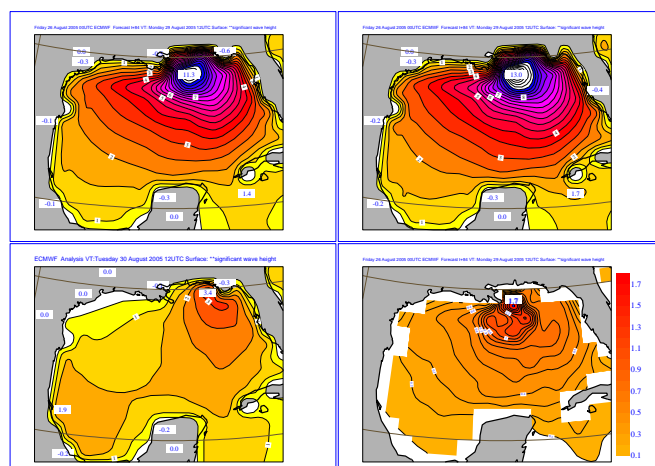


Figure 9: Impact of sea state dependent heat fluxes on the evolution of the wave height field for hurricane Katrina. Forecast step is 84 hours verifying on 2005082912. Upper left panel shows the control simulation, upper right panel shows the experiment and the lower right panel shows the difference between control and experiment. Sea state effects increase maximum wave height by 1.5-2 m.

The Figs. 8 and 9 show results of a  $T_{511}$  simulation with the IFS for surface pressure and significant wave height and the differences between the experiment (with seastate dependent thermal roughness) and control. Impact is quite substantial.

I continued the work on the impact of sea state dependent heat fluxes by running a data assimilation and forecast experiment with the  $T_{799}$  version of the ECMWF model over the period of the 8<sup>th</sup> of August 2007 until the 11<sup>th</sup> of September. I have chosen this period because it is known that sea surface temperature effects play an important role in weather forecasting in this time of the year. Near the sea surface, improvements in forecast skill of geopotential height, temperature and significant wave height were found, but the impact vanished rapidly away from the surface. Sometimes the improvements were quite substantial as follows from a plot of the anomaly correlation of forecast significant wave height over the North Pacific shown in Fig. 10. However, this impact is most likely not representative as it is known from experience that in the summertime

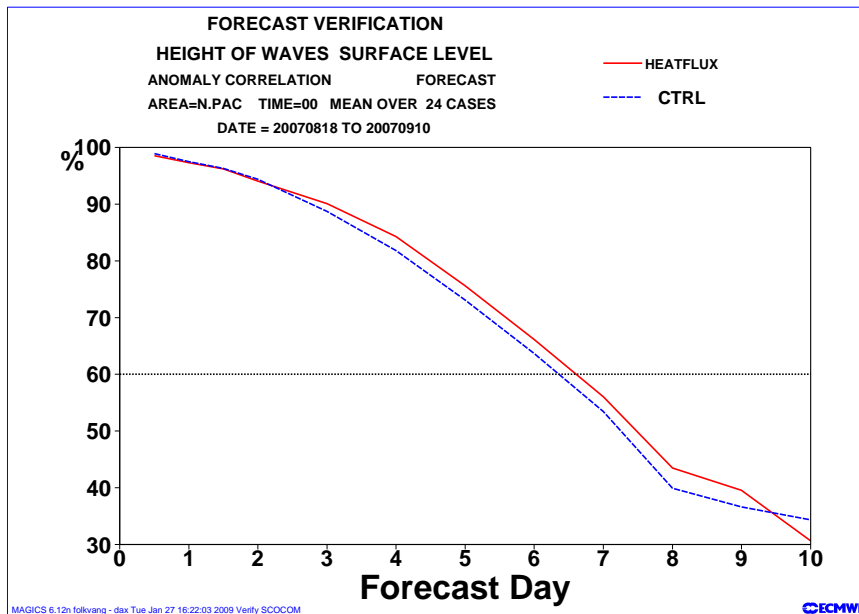


Figure 10: Anomaly correlation of forecast significant wave height as function of forecast time for the Northern Pacific. Shown are scores obtained with sea state dependent heatfluxes and without (CTRL).

weather and sea state forecasting over the North Pacific may show a very sensitive dependence on the initial conditions.

## 4 Wave breaking and the mixed layer

Nowadays the role of breaking ocean waves and its contribution to the surface current and mixing is well-understood (Craig and Banner, 1994; Terray *et al.*, 1999). Near surface dissipation is closely related to the sea state. It are the breaking waves that dump energy in the ocean column and there is no direct correspondence between surface wind and breaking, hence there is no direct relation between energy flux and local wind. A more extensive and more detailed discussion of the role of breaking waves and how to implement their effects in a coupled atmosphere, ocean-wave, ocean circulation model is given in Janssen *et al.* (2004).

In the context of ocean waves the energy flux  $\Phi_{oc}$  and the momentum flux  $\tau_{oc}$  into the ocean are given by

$$\tau_{oc} = \left. \frac{\partial \mathbf{P}}{\partial t} \right|_{diss} = \int d\omega d\theta \frac{\mathbf{k}}{\omega} S_{ds}, \quad \Phi_{oc} = \left. \frac{\partial E}{\partial t} \right|_{diss} = \int d\omega d\theta S_{ds}. \quad (14)$$

Since the dissipation term scales like  $\omega^2 F(\omega)$  the integrals for momentum and energy flux are mainly determined by the high-frequency part of the spectrum. But, because of the extra factor  $k/\omega$ , the momentum flux is, compared to the energy flux, to a larger extent determined by the high frequencies.

The timescales for growth and dissipation of the high frequency part of the spectrum are short and therefore, in practice, the high-frequency part of the ocean wave spectrum is in *equilibrium* with the wind. This means that *wind input and dissipation balance* for these high frequencies. As a consequence, on average, it is a fair approximation to parametrize the momentum flux into the ocean by means of the local stress, but this does not hold for the energy flux (as they are to some extent determined by the longer waves which are not always in equilibrium with the wind). This is illustrated by two examples obtained from Janssen *et al.* (2004): The first

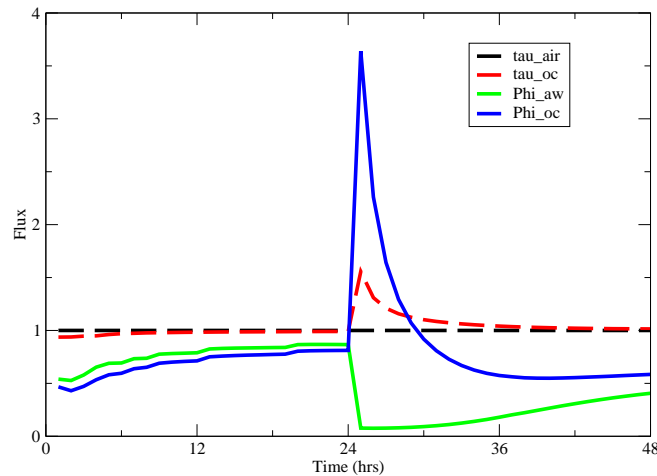


Figure 11: Evolution in time of normalized momentum flux and energy flux to the ocean for the case of a passing front after 24 hrs. The momentum flux has been normalized with  $\rho_a u_*^2$ , while the energy flux has been normalized with  $m \rho_a u_*^3$ , where  $m = 5.2$ .

one is a single grid-point run which mimics the passage of a frontal system. Hence, after one day of a constant wind of 18 m/s, the wind turns by  $90^\circ$  and drops to 10 m/s. In the second example we calculated the fluxes from an actual wave model run for the month of January 2003 and determined the monthly mean. Here the momentum fluxes are scaled with the local stress  $\rho_a u_*^2$ , while the energy flux is scaled by  $m \rho_a u_*^3$  where  $m = 5.2$  which is the mean value from the monthly run.

In Fig. 11 I present results for normalized momentum flux and normalized energy flux for the case of the passage of a front. In agreement with the previous discussion which pointed out that the momentum flux is mainly determined by the high-frequency part of the spectrum, it is seen that to a good approximation the momentum flux going into the ocean equals the momentum flux going into the surface gravity waves. Hence, the momentum flux into the ocean is mainly determined by the local stress. The picture for the energy flux is, however, entirely different. For steady winds there is only a small difference between energy flux into the waves ( $\Phi_{aw}$ ) and energy flux into the ocean ( $\Phi_{oc}$ ) as happens for the first 24 hours of the single grid-point run. However, when the frontal system passes the flux  $\Phi_{oc}$  normalized by the local estimate  $m \rho_a u_*^3$  increases by a factor of three. This overshoot is well understood. Although the wind turns and drops, the ocean waves are still steep, therefore this is still a considerable amount of wave energy being dissipated. The 'delayed' reaction by the waves lasts in this instant for over three hours. As a consequence, parametrizing the energy flux into the ocean in terms of the local stress or local wind, which is nowadays common practice, is expected to be a poor approximation of reality.

This finding has even consequences for the monthly average of the energy flux. In areas where there is high

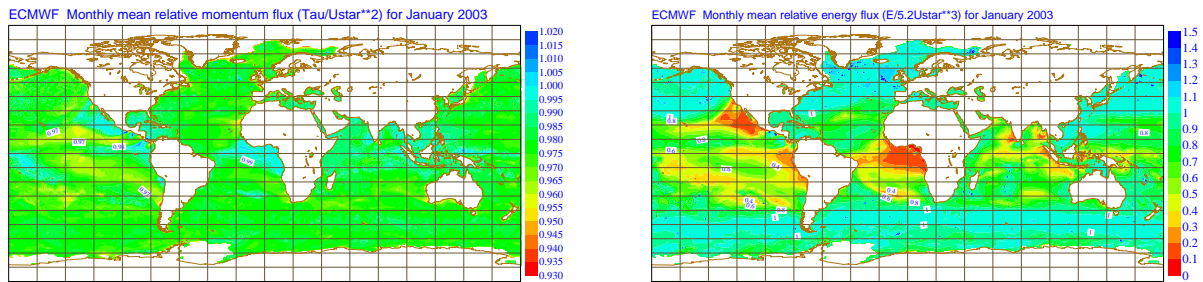


Figure 12: Left Panel: Monthly mean of momentum flux into the ocean, normalized with the atmospheric stress. Right Panel: Monthly mean of energy flux into the ocean, normalized with  $m\rho_a u_*^3$  where  $m \simeq 5.2$ . In both panels the period is January 2003.

variability in the weather accompanied by the passage of frontal systems (e.g. in the storm tracks of the Northern and Southern hemisphere) I would expect a higher normalized energy flux  $\Phi_{oc}/m\rho_a u_*^3$  than when the weather is steady and has hardly no variability in wind speed and direction (e.g. in the areas where the Trade winds prevail). This is nicely supported by Fig. 12 which shows the monthly average of normalized energy flux and momentum flux. In addition, it is clear that to a good approximation the momentum flux into the ocean may be parametrized in terms of the local friction velocity of air.

## 5 Conclusions

My conclusions are the following:

- Two-way interaction of winds and waves results in a realistic distribution of the drag for a hurricane. A maximum in the drag is automatically generated because for extremely young sea state there are relatively few waves to exert a drag on the airflow.
- The ratio of the enthalpy (heat and moisture) to the momentum transfer coefficient plays an important role in the development of a hurricane. Wave dynamics affects the heat and moisture transfer and the resulting Dalton and Stanton number show a good agreement with present day parametrizations of observations (e.g. Brut *et al.* (2005)). The wave effect on heat and moisture flux plays an important role in the evolution of extreme events, but overall impact on forecasts (although positive) is fairly small.
- Parametrization of the energy flux into the ocean is not really feasible using the local friction velocity. An estimate based on wave breaking dissipation seems to be more appropriate.

**Acknowledgements** The author thanks Magdalena Balmaseda for providing Fig. 1, and James Edson for permission to use Fig. 3. Support by the ECMWF wave group (Saleh Abhalla, Jean Bidlot and Hans Hersbach) and Øyvind Sætra is greatly appreciated.

## References

A. Brut, A. Butet, P. Durand, G. Caniaux and S. Planton, 2005. Air-sea exchanges in the equatorial area from the EQUALANT99 dataset: Bulk parametrizations of turbulent fluxes corrected for airflow distortion. *Quarterly Journal of the Royal Meteorological Society*, **131**, 2497-2538.

- G. Caulliez, V.K Makin, and V. Kudryavtsev, 2008. Drag of the Water Surface at Very Short Fetches: Observations and Modeling. *J. Phys. Oceanogr.*, **38**, 2038-2055.
- Craig, P.D. and M.L. Banner, 1994. Modeling wave-enhanced turbulence in the ocean surface layer. *J. Phys. Oceanogr.* **24**, 2546-2559.
- J. DeCosmo, K. Katsaros, S. Smith, R. Anderson, W. Oost, K. Bumke, and H. Chadwick (1996), Air-sea exchange of water vapor and sensible heat: The Humidity Exchange Over the Sea (HEXOS) results, *J. Geophys. Res.*, **101(C5)**, 12001-12016.
- Donelan, M.A., 1982. The dependence of the aerodynamic drag coefficient on wave parameters, p381-387 in: Proc. of the first international conference on meteorological and air/sea interaction of the coastal zone; Amer. Meteor. Soc., Boston, Mass.
- Kerry A. Emanuel ,1995. Sensitivity of Tropical Cyclones to Surface Exchange Coefficients and a Revised Steady-State Model incorporating Eye Dynamics, *Journal of the Atmospheric Sciences*, **52**, 3969-3976.
- K. Hasselmann, T.P. Barnett, E. Bouws, H. Carlson, D.E. Cartwright, K. Enke, J.A. Ewing, H. Gienapp, D.E. Hasselmann, P. Kruseman, A. Meerburg, P. Müller, D.J. Olbers, K. Richter, W. Sell, H. Walden, Measurements of wind-wave growth and swell decay during the Joint North Sea Wave Project (JONSWAP), *Dtsch. Hydrogr. Z. Suppl. A* 8(12) (1973) 95p.
- P.A. Hwang, 2005. Temporal and spatial variation of the drag coefficient of a developing sea under steady wind-forcing. *J. Geophys. Res.*, **110**, C07024. doi:10.1029/2005JC002912
- P.A.E.M. Janssen, 1991. Quasi-linear theory of wind wave generation applied to wave forecasting. *J. Phys. Oceanogr.* **21**, 1631-1642.
- P.A.E.M. Janssen, 1997. Effect of surface gravity waves on the heat flux. ECMWF Technical Memorandum no. 239.
- P.A.E.M. Janssen, J.D. Doyle, J. Bidlot, B. Hansen, L. Isaksen and P. Viterbo, 2002: Impact and feedback of ocean waves on the atmosphere. in *Advances in Fluid Mechanics*, **33**, Atmosphere-Ocean Interactions ,Vol. I, Ed. W.Petrie.
- Peter A.E.M. Janssen, Øyvind Sætra, Cecilie Wettre, Hans Hersbach and Jean Bidlot, 2004: Impact of the sea state on the atmosphere and ocean. *Annales Hydrographiques*, **3**, 3.1-3.23.
- Peter Janssen, *The Interaction of Ocean Waves and Wind*, Cambridge University Press, Cambridge, U.K., 2004, 300+viii pp.
- G.J. Komen, P.A.E.M. Janssen, V. Makin, and W. Oost, 1998. On the sea state dependence of the Charnock parameter. *GAOS* **5**, 367-388.
- G.J. Komen, L. Cavaleri, M. Donelan, K. Hasselmann, S. Hasselmann, and P.A.E.M. Janssen, 1994: *Dynamics and Modelling of Ocean waves* (Cambridge University Press, Cambridge), 532 p.
- W.A. Oost, C.M.J. Jacobs, C. Van Oort, 2000. Stability effects on heat and moisture fluxes at sea. *Boundary-Layer Meteorol.*, **95**, 271-302.
- M.D. Powell, 2008. New findings on hurricane intensity, wind field extent and surface drag coefficient behavior. Proceedings of the tenth international workshop on wave hindcasting and forecasting and coastal hazard symposium, North Shore, Oahu, Hawaii, 11-16 November 2007.
- Øyvind Sætra, Jon Albrechtsen and Peter A.E.M. Janssen, 2007. Sea-State-Dependent Momentum Fluxes for Ocean Modeling. *J. Phys. Oceanogr.* **37**, 2714-2725.
- Ann-Sofi Smedman, Ulf Sahle, Erik Högström, and Cecilia Johansson, 2007. Critical re-evaluation of the bulk transfer coefficient for sensible heat over the ocean during unstable and neutral conditions. *Quarterly Journal of the Royal Meteorological Society*, **133**, 227-250.

S.D. Smith, R.J. Anderson, W.A. Oost, C. Kraan, N. Maat, J. DeCosmo, K.B. Katsaros, K.L. Davidson, K. Bumke, L. Hasse and H.M. Chadwick, 1992. Sea surface wind stress and drag coefficients: the HEXOS results. *Boundary Layer Meteorol.* **60**, 109-142.

E.A. Terray, W.M. Drennan, and M.A. Donelan, 1999. The vertical structure of shear and dissipation in the ocean surface layer. *The wind-driven air-sea interface*, M.L. Banner, Ed., School of Mathematics, The University of New South Wales, Sydney, 239-245.